EurJIC
European Journal of Inorganic Chemistry

A Journal of ChemPubSoc Europe

Accepted Article

Title: Complexes Containing a Phenol-Platinum(II) Hydrogen Bond: Synthons for Supramolecular Self-Assembly and Precursors for Hydridoplatinum(IV) Complexes

Authors: Ava Behnia, Mahmood Azizpoor, Paul D. Boyle, and Richard J. Puddephatt

To be cited as: *Eur. J. Inorg. Chem.* 10.1002/ejic.201900480

Link to VoR: http://dx.doi.org/10.1002/ejic.201900480

WILEY-VCH

Complexes Containing a Phenol-Platinum(II) Hydrogen Bond: Synthons for Supramolecular Self-Assembly and Precursors for Hydridoplatinum(IV) Complexes

Ava Behnia,[a] Mahmood Azizpoor Fard,[a] Paul D. Boyle[a] and Richard J. Puddephatt*[a]

[a] *Department of Chemistry, The University of Western Ontario, London, Canada N6A 5B7*

E-mail: pudd@uwo.ca

Abstract

The cycloneophylplatinum(II) complexes [Pt($CH_2CMe_2C_6H_4$)(κ^2-NN'-2-$C_5H_4NCH_2$-NH-R], R = 2-C_6H_4OH, **1**; R = 3-C_6H_4OH, **2**; R = 4-C_6H_4OH, **3**, and [Pt($CH_2CMe_2C_6H_4$)(κ^2-NN'-2-C_5H_4NCH=N-2-C_6H_4OH)], **4**, are reported. The structures of **1** and **4** each contain an intramolecular OH···Pt hydrogen bond, while complex **3** contains an intermolecular OH···Pt hydrogen bond and forms a new type of supramolecular polymer. In contrast, the complex [$PtCl_2$(κ^2-NN'-2-C_5H_4NCH=N-2-C_6H_4OH)], **5**, forms a dimer through intermolecular OH···ClPt hydrogen bonding. Reaction of complex **4** with HCl or HBr occurs by oxidative addition to give hydridoplatinum(IV) complexes [PtHX($CH_2CMe_2C_6H_4$)(κ^2-NN'-2-C_5H_4NCH=N-2-C_6H_4OH)], **6**, X = Cl; **7**, X = Br. The sequential formation of isomers of these compounds is interpreted in terms of a proposed reaction mechanism.

Introduction

In many catalytic reactions involving platinum or its complexes, the interaction of a platinum atom with a hydroxylic solvent or reagent is critically important. It may involve formation of a non-classical O-H···Pt hydrogen bond,[1] formation of a reactive hydridoplatinum intermediate,[2] or a long range interaction involving another reagent such as dioxygen.[3] In forming a non-classical O-H···Pt hydrogen bond, the electron-rich platinum atom can be considered to act as a 2-electron donor while maintaining its oxidation state,[1,4] while hydride formation typically occurs by oxidative addition.[2] The intermolecular O-H···Pt hydrogen bond can also participate in self-assembly to form polymeric complexes in the crystalline state.[1] Appended phenol substituents are known to form intramolecular O-H···Pt(II) hydrogen bonds (Scheme 1), but these do not lead to

oxidative addition of the O-H bond to make hydridoplatinum(IV) complexes, and no intermolecular equivalents are known.[1,5] Indeed there has been doubt that these hydrogen bonds would ever be considered as structure-directing elements for extended supramolecular arrays.[1e] One example is known in which a platinum(II) complex with an NH··Pt hydrogen bond from an appended pyridinium group is in equilibrium with the hydrido(pyridine)platinum(IV) complex,[6] but no OH··Pt(II) and O-Pt(IV)-H isomers appear to be known.

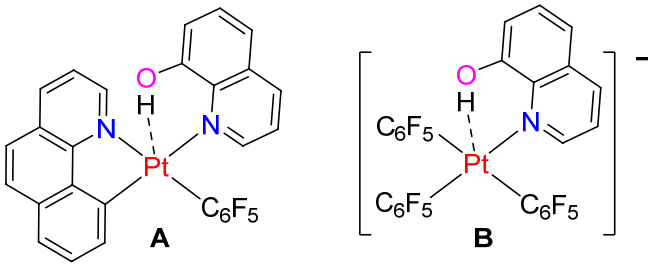

Scheme 1. Pt(II)-phenol hydrogen bonds.

This article reports the synthesis and structure of three new complexes containing phenolic OH··Pt(II) hydrogen bonds, including the first example of a supramolecular polymer based on intermolecular OH··Pt hydrogen bonds and an estimate of the bond strength. It also investigates the formation of hydridoplatinum(IV) complexes from the platinum(II) precursor complexes.

Results and Discussion

The ligands used in this work are shown in Scheme 2. They contain a pyridyl group and an amine (**L1** – **L3**) or imine group (**L4**) that allow the ligands to chelate to platinum(II). They also contain an appended phenol group that can be placed in the *ortho*, *meta* or *para* position and which, when deprotonated, can act as a third donor.[7] Dimethylplatinum(II) complexes with these ligands are electron-rich and are very easily oxidized; they have not been structurally characterized.[8] Cationic monomethylplatinum(II) complexes, such as [PtMe(SMe_2)(**L1**)]Cl, are also known and they form supramolecular polymers through OH..Cl and NH..Cl hydrogen bonding, and do not contain OH··Pt hydrogen bonds.[9] The new electron-rich cycloneophylplatinum(II) complexes **1** – **4** were prepared by reaction of the precursor complex [$Pt_2(CH_2CMe_2C_6H_4)_2(\mu\text{-}SMe_2)_2$][10] with the corresponding ligands **L1** – **L4**, with

displacement of the weakly bound dimethylsulfide ligands (Scheme 2). The new complexes were characterized spectroscopically and complexes **1**, **2** and **3** were shown to contain OH··Pt hydrogen bonds by X-ray structure determinations.

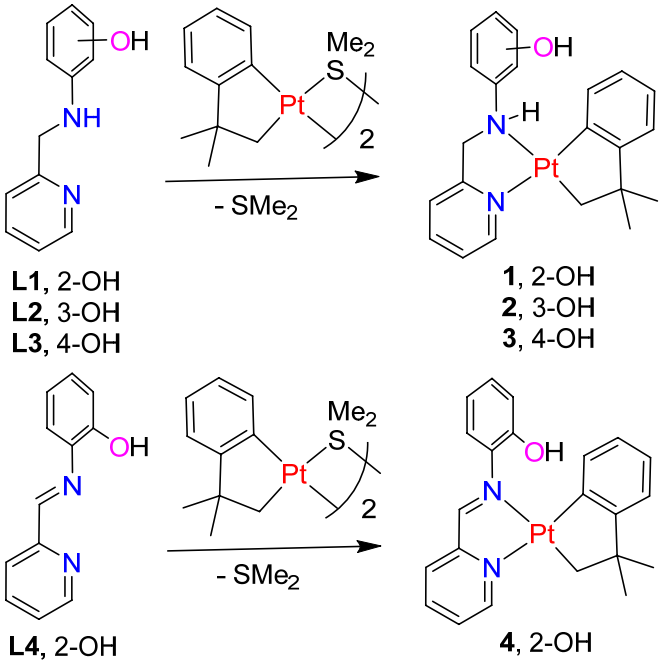

Scheme 2. The ligands and their cycloneophylplatinum(II) complexes.

The structures of the 2-hydroxyphenyl derivatives **1** and **4** are shown in Figure 1. In each case, the platinum(II) center is square planar with the aryl and pyridyl groups mutually *trans*. This stereochemistry is expected because it avoids unfavorable steric interactions between the roughly co-planar aryl and pyridyl groups.[10] However, the main feature of interest is the presence of an OH..Pt hydrogen bond in each complex. The structural data for complex **1** were of high quality and it was possible to locate and refine the OH hydrogen atom position. The parameters O(1)-H(1A) 0.84(5) Å, Pt(1)··H(1A) 2.37(3) Å, O(1)-H(1A)··Pt(1) 162(2)°, are similar to those for complex **A** (Scheme 2, O-H 0.91(4) Å, Pt··H 2.10(4) Å, O-H··Pt 162(4)°], clearly showing the presence of the OH··Pt bond.[5] The Pt··O distance in **4** [Pt(1)··O(1) 3.23(1) Å] is slightly higher than in **1** [Pt(1)··O(1) 3.175(1) Å], perhaps indicating a slightly weaker OH..Pt hydrogen bond; the difference probably arises from geometrical constraints of the imine group in **4**.

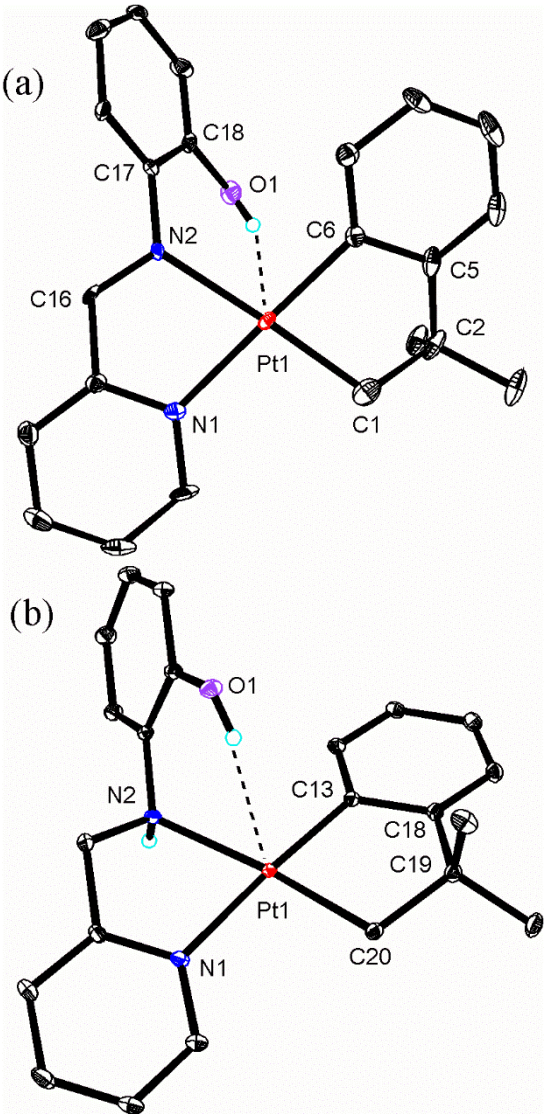

Figure 1. Structures of complexes (a) **4** and (b) **1**, showing 30% probability ellipsoids. (a) Pt(1)C(1) 2.035(5), Pt(1)C(6) 1.995(5), Pt(1)N(1) 2.110(4), Pt(1)N(2) 2.125(4), Pt(1)···O(1) 3.23(1) Å; C(1)Pt(1)C(6) 80.2(2), N(1)Pt(1)N(2) 77.3(1)°. (b) Pt(1)C(13) 1.9954(11), Pt(1)C(20) 2.0228(12), Pt(1)N(1) 2.1056(10), Pt(1)N(2) 2.2075(11), Pt(1)···O(1) 3.175(1), Pt(1)···H(1) 2.37 Å; C(13)Pt(1)C(20) 81.38(5), N(1)Pt(1)N(2) 78.04(4)°.

The structure of complex **3** is shown in Figure 2. The stereochemistry at platinum(II) is similar to that found in **1** and **4**, with the aryl and pyridyl groups mutually *trans*. In this case, formation of an intramolecular OH···Pt bond is impossible but an intermolecular bond is formed instead. The short Pt···O contact of 3.14(1) Å clearly represents the OH···Pt bond; the distance is somewhat shorter than in **1** and **4**. The hydrogen atom was located and the associated distance Pt···H = 2.28(8) Å and angle Pt···H-O = 155(7)° are similar to

the values found for complex **1**. Propagation of this motif gives a supramolecular polymeric structure, with chains running parallel to the x-axis. The molecule is chiral at the amine nitrogen atom, so each individual polymer chain is isotactic. The space group is not chiral and so there are equal numbers of chains with *RRR* and *SSS* chirality. The complex with an electron-rich metal center and a ligand with an appended 4-hydroxyphenyl group is particularly well suited for making one-dimensional supramolecular polymers, and it should be possible to prepare many other examples.

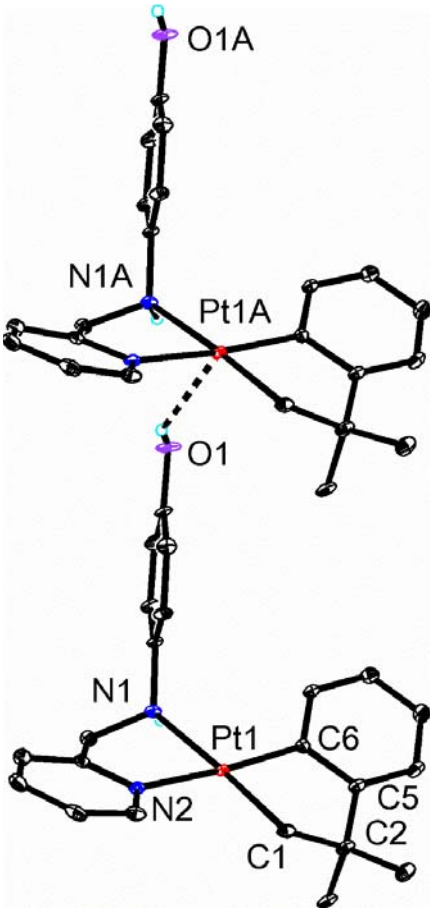

Figure 2. The structure of complex **3**, showing 30% probability ellipsoids. Selected bond parameters: Pt(1)C(1) 2.036(6), Pt(1)C(6) 1.985(6), Pt(1)N(1) 2.205(5), Pt(1)N(2) 2.097(5), Pt(1A)···O(1) 3.14(1) Å; C(1)Pt(1)C(6) 80.7(2), N(1)Pt(1)N(2) 79.6(2)°. Symmetry equivalent atoms: x, y, z; x-1, y, z.

In order to compare the above structures with that of a more typical inorganic platinum(II) complex, we have prepared the dichloroplatinum(II) derivative [$PtCl_2$(**L4**)], **5** (Scheme 3). Complex **5** is a sparingly soluble yellow solid, prepared either by ligand

displacement from $[PtCl_2(SMe_2)_2]$ or by cleavage of the cycloneophylplatinum group from complex **4** by excess HCl. The structure of complex **5** is shown in Figure 3. There is no OH··Pt hydrogen bond but there is a long CH··Pt interaction (Pt··H 2.66 Å, C-H..Pt 157°) which could indicate a weak hydrogen bond.[1] Two square planar units are connected to form a supramolecular dimer by OH··Cl hydrogen bonding, with O(1)··Cl(1A) = Cl(1)··O(1A) = 3.187(2) Å. In this case, it seems that the chloride ligand is a better hydrogen bond acceptor than the platinum(II) center, which is less electron-rich than in the cycloneophyl complexes.

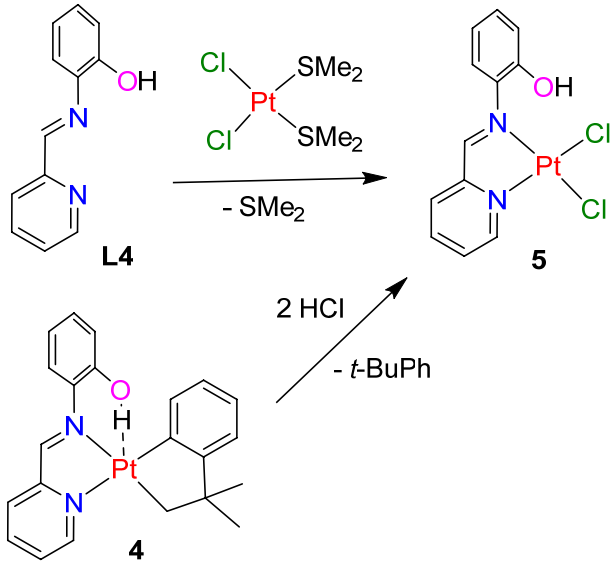

Scheme 3. Synthesis of complex **5**.

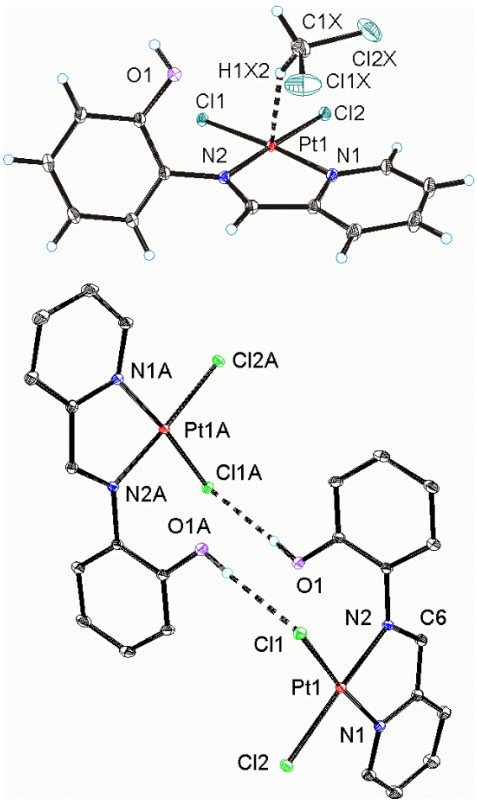

Figure 3. Structure of complex **5**, showing 30% probability ellipsoids: above a solvated molecule; below, a supramolecular dimer. Selected bond parameters: Pt(1)N(1) 2.0098(15), Pt(1)N(2) 2.0142(15), Pt(1)Cl(1) 2.2874(6), Pt(1)Cl(2) 2.3014(6), O(1)..Cl(1A) 3.187; N(1)Pt(1)N(2) 80.08(6), Cl(1)Pt(1)Cl(2) 89.456(16)°. Symmetry equivalent atoms: x, y, z; 1-x, 1-y, 2-z.

The NMR spectra of the complexes **1** – **3** were unremarkable. The presence of the chiral center at nitrogen leads to no symmetry and this is clearly seen in the ^{1}H NMR spectra. For example, in the ^{1}H NMR spectrum of complex **1**, the CH_2 protons of the cycloneophyl group are non-equivalent and appeared as two sharp doublets at δ 2.60 and 2.02, with geminal coupling ^{2}J(HH) = 10 Hz. In contrast, the ^{1}H NMR spectrum of complex **4** at room temperature gave no visible resonance for these CH_2 protons; however, at -20°C the expected resonances were observed at δ 3.38 and 2.48, with geminal coupling ^{2}J(HH) = 12 Hz. The coalescence temperature is 25°C and, because of the significant chemical shift difference, the resonance is too broad to observe. The data are interpreted according to the mechanism in Scheme 4. The hydrogen bonded ground

state structure **4** has no symmetry and, for the molecule to gain an effective plane of symmetry to make the CH^aH^b protons equivalent, the hydrogen bond must break to allow rotation of the 2-hydroxyphenyl group to form the hydrogen bond on the opposite side of the square plane via the intermediate **4*** (Scheme 4). The activation energy $\Delta G^{\dagger}$ is estimated as 55 kJ mol^{-1} at 298K from the Eyring equation (see experimental) and could be taken as an upper limit of the OH··Pt bond energy. The NMR spectrum of **4** showed the presence of a minor component, suggested to be the isomer with the CH_2 group *trans* to pyridine, **4'**, but it was never present in more than 5% abundance.

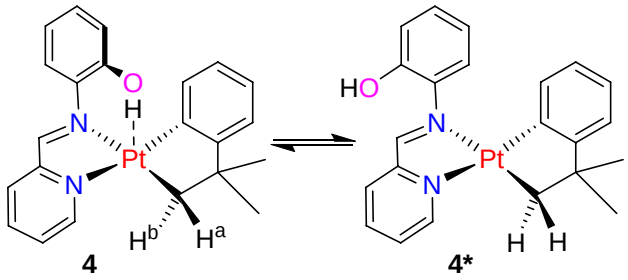

Scheme 4. Inversion of the hydrogen bond structure in complex **4**.

DFT calculations (see experimental for details) give some insight into the nature of the hydrogen bonds (Figure 4). In complex **4**, the OH hydrogen atom is directed towards the platinum atom and the main interaction is with the filled d_z^2 orbital of the electron-rich platinum(II) center (Figures 4a, 4b). In contrast, the OH hydrogen atom in complex **5** is directed towards the adjacent chloride ligand and the main interaction is with one of the filled p_π orbitals of the chlorine atom (Figures 4c, 4d), which are at higher energy than the d_z2 orbital of the less electron-rich platinum(II) center. In the solid state structure, a closer OH··Cl approach is possible and the dimer structure is formed (Figure 3). The hydrogen bond interaction in complex **1** (Figures 4e, 4f) is similar to that in complex **4**, involving the d_z^2 orbital of platinum(II). In complex **3**, no intramolecular hydrogen bonding is possible (Figures 4g, 4h). It is noteworthy that the orbital with mostly $5d_z2$ character lies at -6.27 eV in **1** but at -5.74 eV in **4**, reflecting the stabilization of this orbital by the hydrogen bonding in **1**. All of the DFT calculations support the view that the OH..Pt hydrogen bond strength depends on the energy of the filled d_z^2 orbital, which acts as the hydrogen bond acceptor.[4,5]

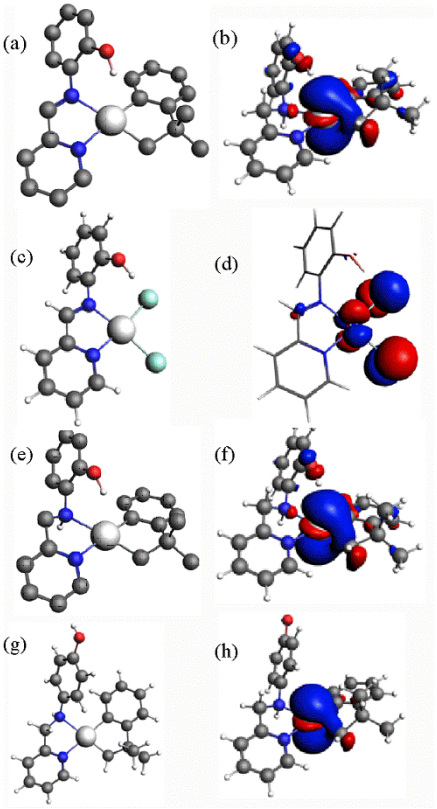

Figure 4. Calculated structures and H-bond frontier orbitals: (a), (b), complex **4**; (c), (d), complex **5**; (e), (f), complex **1**; (g), (h) complex **3**. For (b), (f), (h), the filled orbital has mostly platinum $5d_{z2}$ character while, for (d) it has mostly Cl $3p_z$ character.

The platinum(II) complexes **1** – **4** did not equilibrate with their potential hydridoplatinum(IV) isomers in solution. DFT calculations predict that the isomerization of complex **4** to the platinum(IV) complex [PtH($CH_2CMe_2C_6H_4$)(κ^3-NN'O-2-C_5H_4NCH=N-2-C_6H_4O)] is unfavorable by 68-83 kJ mol^{-1}, depending on the isomer formed, so this is not surprising. However, platinum(IV) hydride complexes were formed by reaction of **4** with strong acids HCl or HBr and are expected to have the structure [PtHX($CH_2CMe_2C_6H_4$)(κ^2-NN'-2-C_5H_4NCH=N-2-C_6H_4OH)], **6**, X = Cl; **7**, X = Br . The reagent HCl was generated in CD_2Cl_2 solution by reaction of Me_3SiCl with water and it was added to a solution of complex **4** in CD_2Cl_2 at -60°C and ^1H NMR spectra were recorded as the solution was warmed to room temperature. Four hydride complexes were detected, as illustrated in Figure 5. At -30°C (Figure 5a), the dominant hydride resonance was at δ −19.62, $^1J_{PtH}$ = 1466 Hz (isomer **6a**), at 25°C (Figure 5b) the dominant hydride

resonance was at δ −19.51, $^1J_{PtH}$ = 1400 Hz (isomer **6b**), and after one day at 25°C (Figure 5c) the dominant hydride resonance was at δ −19.17, $^1J_{PtH}$ = 1380 Hz (isomer **6c**). Under conditions where **6b** was dominant, a complete ^{1}H NMR analysis was possible. A fourth hydride resonance was observed at δ −20.19, $^1J_{PtH}$ = 1484 Hz (isomer **6d**, indicated by an asterisk in Figure 5b), but it was never the major complex present. By integration against an internal standard, the total yield of hydride complexes was determined to be essentially quantitative at 25°C, but it was reduced to about 70% after one day and to zero after one week, with parallel formation of complex **5** (Scheme 3). If the hydride complexes were generated in CD_2Cl_2 solution as above, with isolation by evaporation of the solvent, washing of the residue with ether to remove organosilicon compounds, drying under vacuum and redissolving in CD_2Cl_2, the same hydride complexes **6a** – **6d** were detected by their hydride resonances but the product mixture contained about 80% of complex **4** by ^{1}H NMR analysis. This indicates that HCl addition to complex **4** to give **6a** – **6d** is reversible, and that HCl loss regenerates complex **4**. Attempts to grow crystals from the mixture of hydride complexes at low temperature were unsuccessful so unambiguous assignment of the isomer structures was not possible. The reaction of complex **4** with HBr occurred in a similar way to give isomers of [PtHBr($CH_2CMe_2C_6H_4$)(**L4**)], **7**, formed in the sequence **7a** [δ −19.66, $^1J_{PtH}$ = 1453 Hz], **7b** [δ −19.56, $^1J_{PtH}$ = 1395 Hz], **7c** [δ −19.16, $^1J_{PtH}$ = 1356 Hz], with minor isomer **7d** [δ −20.06, $^1J_{PtH}$ = 1444 Hz]. The *trans*-influence series is imine, pyridine > Cl^-, Br^-, so the data are consistent with the initially formed isomer **6a** or **7a** having hydride *trans* to halide while the later isomers **6b**, **6c**, **7b**, **7c** have hydride *trans* to a nitrogen-donor ligand.[11] A hydride *trans* to CH_2 or C_6H_4 would give a much lower coupling constant,[2] so only isomers with the *fac*-$PtHC_2$ coordination need to be considered.

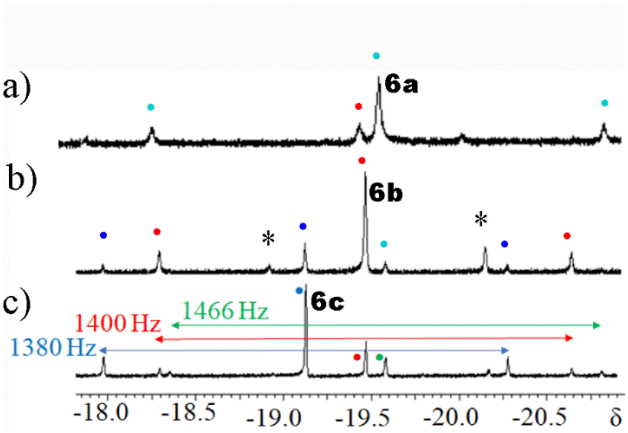

Figure 5. ^{1}H NMR spectra (400 MHz) of complex **6** in the hydride region: a) at -30°C; b) at 25°C; c) after 24 h. at 25°C.

Complexes **1** – **3** also reacted with HCl to give mixtures of hydridoplatinum(IV) complexes but these were not sufficiently stable to allow characterization. For example, reaction of complex **1** in CD_2Cl_2 with HCl gave isomers of [PtHCl($CH_2CMe_2C_6H_4$)(κ^2-NN'-2-$C_5H_4NCH_2$-NH-2-C_6H_4OH)], **8**. Five hydride resonances were observed [δ −19.63, $^{1}J_{PtH}$ = 1340 Hz; -19.90; -20.37, $^{1}J_{PtH}$ = 1687 Hz; -20.91; -21.13] but ^{195}Pt couplings were only resolved for the two most intense peaks. Complete loss of these peaks occurred in a few hours at room temperature. Because the hydridoplatinum(IV) complexes from ligands **L1** – **L3** are chiral at both the amine and platinum(IV) centers, more isomers are possible than with **L4**, and the low thermal stability hinders more complete characterization.

The sequential formation of isomers from the reaction of complex **4** with HCl or HBr is unusual and some DFT calculations were carried out on potential products in order to gain further insight (Scheme 5, Figure 6). There are six potential geometrical isomers of complex **6** having the preferred *fac*-$PtHC_2$ coordination, labeled **P1** – **P6** in Scheme 5 and Figure 6. They are all expected to have intramolecular OH···Cl hydrogen bonds (Figure 6), though these are not shown in Scheme 5, for clarity. Their energies with respect to complex **4** + HCl lie in the range -80 to -100 kJ mol^{-1}, so the oxidative addition is favorable (Figure 6). In terms of mechanism, the protonation of complex **4** is expected to form the 5-coordinate cationic square pyramidal intermediate **I1** and then chloride coordination at the vacant site would give product isomer **P1**. Isomerization of **P1** is

likely to involve chloride dissociation to regenerate intermediate **I1**, followed by rearrangement and recoordination of chloride. The isomerization of the 16-electron platinum(IV) intermediates is thought to occur by migration of an equatorial group to the vacant axial site while the axial group moves to the vacated equatorial site, by way of a pinched trigonal bipyramidal intermediate.[10,12] In this mechanism, **I1** can rearrange to **I2** or **I3** and chloride coordination can then give **P2** or **P3**. Similarly, intermediates **I2** and **I3** can isomerize back to **I1** or go on to form **I4** and **I5** respectively, and chloride coordination can then give products **P4** and **P5**. Finally, isomerization of **I4** or **I5** can give **I6** and this can give **P6**. Of course, **I6** and then **P6** might also be formed by direct reaction of HCl with the minor isomer of complex **4** (**4'**).

10.1002/ejic.201900480

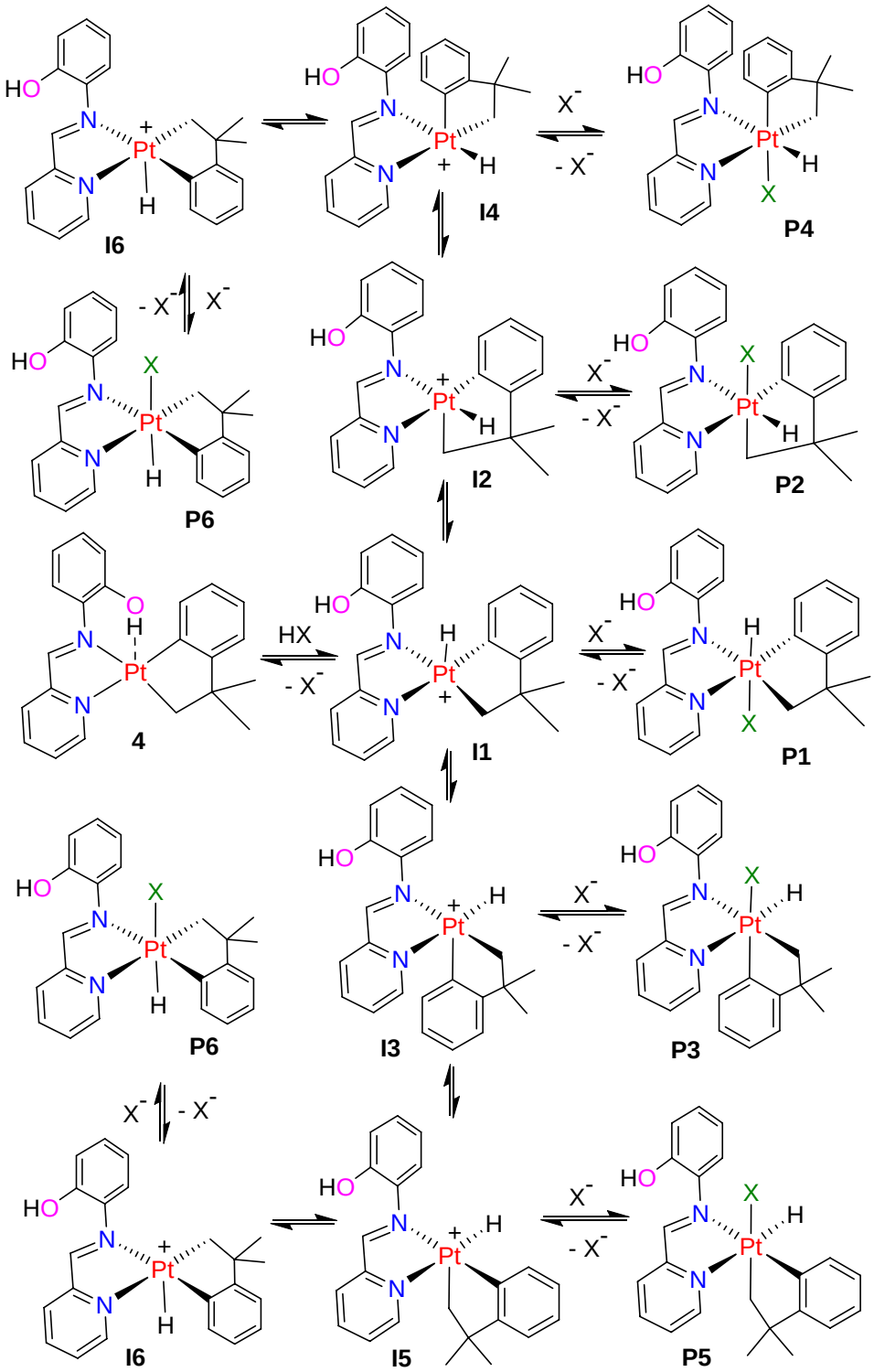

Scheme 5. The six potential isomers **P1** – **P6** by oxidative addition of HX to complex **4**, and their likely formation through intermediates **I1** – **I6**.

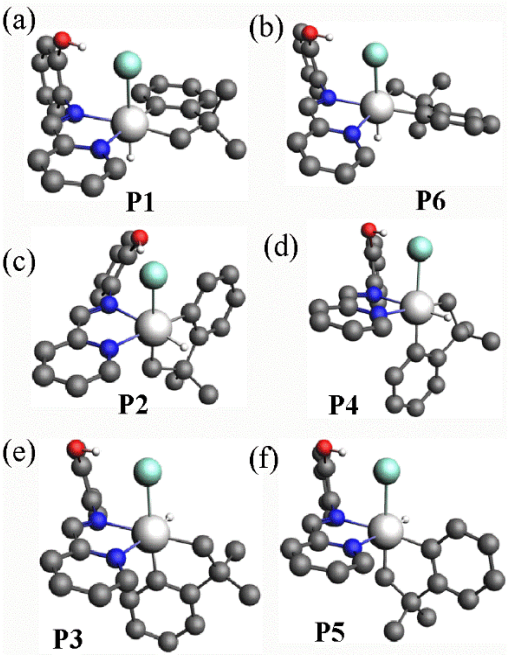

Figure 6. Calculated structures for the potential isomers of [PtHCl($CH_2CMe_2C_6H_4$)(κ^2-NN'-2-C_5H_4NCH=N-2-C_6H_4OH)], **6**. Relative energies with respect to **4** + HCl are: **P1**, **P6** -80; **P2**, **P3** -89, **P5** -90, **P4** -100 kJ mol^{-1}.

The final challenge is to correlate the four observed structures **6a** – **6d** (X = Cl) or **7a** – **7d** (X = Br) with four of the six possible structures **P1** – **P6** of [PtHX($CH_2CMe_2C_6H_4$)(κ^2-NN'-2-C_5H_4NCH=N-2-C_6H_4OH)] (Scheme 6). Precedents for *trans* oxidative addition of HX, as a result of kinetic control (Scheme 5), predict that the first formed isomer from **4** should be **P1**, and the NMR data fully support the assignment of this structure to the first formed isomer **6a** or **7a**.[2] According to Scheme 5, the first product of isomerization should have structure **P2** or **P3** and so the observed complex **6b** or **7b** is expected to have one of these two structures. Isomers **P2** and **P3** are calculated to have the same energy so the calculations do not aid the assignment, and the assignment of **6b**, **7b** to have structure **P2** is therefore tentative. The isomer **P4** is calculated to be most stable so the more stable observed isomer **6c** or **7c** is likely to have this structure. Finally, complex **6d** or **7d** is proposed to have the structure **P6**. Complex **6d**, **7d** appears to be formed primarily by direct reaction of complex **4'** with HX. It might also be formed by isomerization of **P4** (Scheme 5), though this reaction is calculated to be unfavorable.

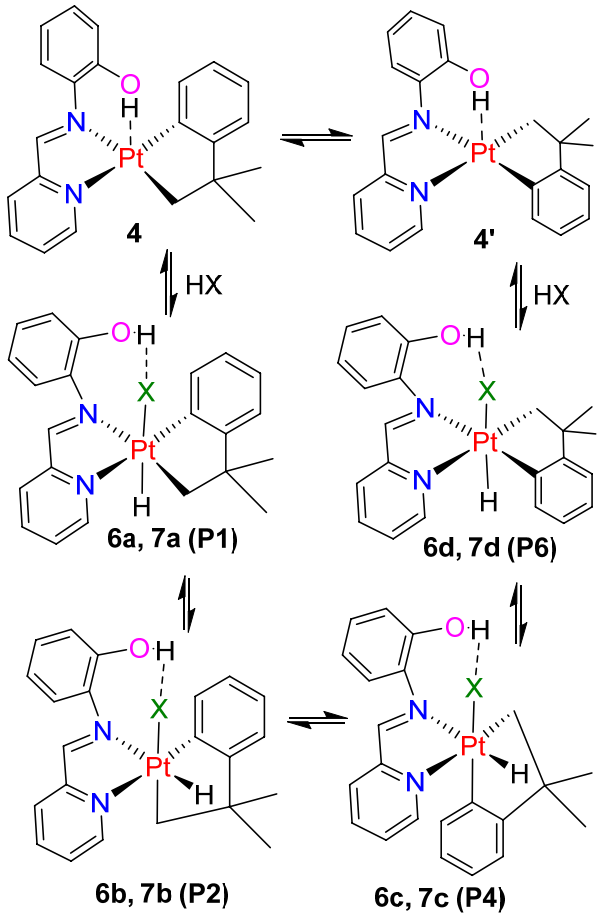

Scheme 6. Proposed structures of complexes [PtHCl($CH_2CMe_2C_6H_4$)(κ^2-NN'-2-C_5H_4NCH=N-2-C_6H_4OH)], **6a** – **6d** (X = Cl), **7a** – **7d** (X = Br).

Conclusions

New examples of phenol based OH···Pt hydrogen bonds are established in the structures of **1**, **3** and **4**, and DFT calculations support the view that a high energy platinum $5d_{z^2}$ orbital is most important in promoting such bonds.[4,5] The ligands used in this work are easily modified and so are expected to yield further examples. For example, the phenol acidity could be modified by introducing appropriate substituents and this could be used to tailor the strength of the unconventional hydrogen bonds. The demonstration in the structure of complex **3** that the hydrogen bonds can support formation of a supramolecular polymer is particularly significant. The oxidative addition of acids HX (X = Cl or Br) to complex **4** occurs in an unexpected way to give sequential formation of

isomeric hydridoplatinum(IV) complexes, and a mechanism to account for this unusual behavior is proposed.[2]

Experimental

IR spectra were recorded by using a Perkin Elmer UATR TWO FTIR spectrometer. NMR spectra were recorded using a Varian Inova 600 MHz spectrometer. Complete assignments of each compound were aided by the use of $^{1}H–^{1}H$ gCOSY, $^{1}H–^{13}C$ HSQC, and $^{1}H–^{13}C$ HMBC experiments and are reported using the labeling scheme in Scheme 7. The activation energy for the inversion of the hydrogen bond in complex **4** was estimated from the variable temperature ^{1}H NMR spectra by using the Eyring equation.[13] The complex $[Pt_2(CH_2CMe_2C_6H_4)_2(\mu\text{-}SMe_2)_2]$ and ligands **L1** – **L4** were synthesized according to the literature procedures.[7,10a] MALDI-TOF mass spectra were collected using an AB Sciex 5800 TOF/TOF mass spectrometer using pyrene or anthracene as the matrix in a 20:1 matrix:substrate molar ratio. Single-crystal X-ray diffraction measurements were made using a Bruker APEX-II CCD diffractometer with graphite-monochromated Mo Kα (λ = 0.71073 Å) radiation. Single crystals of the complexes were immersed in paraffin oil and mounted on MiteGen micromounts. The structures were solved using dual space methods and refined by the full-matrix least-squares procedure of SHELXL. Crystallographic data are given in the crystallographic information files. The DFT calculations were carried out (gas phase only) using the B1LYP functional with double-zeta basis set and first-order scalar relativistic corrections, as implemented in ADF-2017.[14]

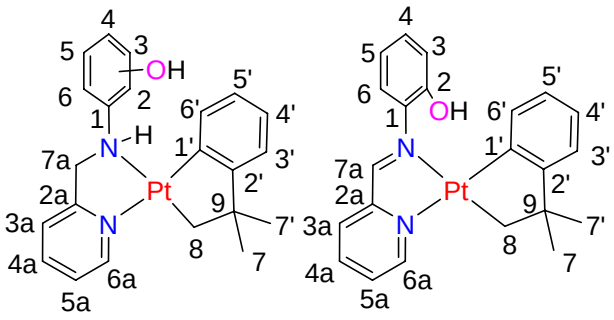

Scheme 7. NMR labelling scheme.

[Pt(CH$_2$CMe$_2$C$_6$H$_4$)(L1)], 1.

To a stirred solution of $[Pt_2(CH_2CMe_2C_6H_4)_2(\mu\text{-}SMe_2)_2]$, (0.196 g, 0.252 mmol) in dry CH_2Cl_2 (15 mL) was added 2-C_5H_4N-CH_2-NH-2-C_6H_4OH, **L1** (0.100 g, 0.504 mmol). An immediate color change from yellow to brown was observed. The reaction mixture was stirred for 2.5 h., the solvent was evaporated under vacuum, and the residue was washed with dry hexane (3 × 2 mL) and dry ether (3 × 2 mL), to give complex **1** as a brown solid (0.172 g, 0.325 mmol, 65%). NMR in CD_2Cl_2 (25°C): δ(^{1}H, 600 MHz) 8.46 (d, 1H, *J* = 5 Hz, *H*6a), 7.85 (dd, 1H, *J* = 8 Hz, 5 Hz, *H*4a), 7.25 (d, 1H, *J* = 8 Hz, *H*3a), 7.19 (t, 1H, *J* = 8 Hz, *H*5a, 1H), 7.02 (t, 1H, *J* = 8 Hz, *H*5), 6.81 (d, 1H, *J* = 8 Hz, *H*6'), 6.77 (t, 1H, *J* = 8 Hz, *H*5', 1H), 6.70-6.72 (m, 2H, *H*4, *H*6), 6.49 (d, 1H, *J* = 8 Hz, *H*3), 6.35 (br dd, 1H, *J* = 12 Hz, 6 Hz, NH), 6.32 (d, 1H, *J* = 8 Hz, *H*3'), 6.20 (t, 1H, *J* = 8 Hz, *H*4'), 4.40 (dd, 1H, *J* = 16 Hz, 6 Hz, *H*7a, 1H), 4.13 (dd, 1H, *J* = 16 Hz, 12 Hz, *H*7a'), 2.60 (d, 1H, *J* = 10 Hz, *H*8), 2.02 (d, 1H, *J* = 10 Hz, *H*8'), 1.37 (s, 3H, *H*7), 1.23 (s, 3H, *H*7'). δ(^{13}C, 151 MHz) 168.66 (*C*2'), 160.72 (*C*2a), 150.47 (*C*2), 147.97 (*C*6a), 140.38 (*C*1'), 137.19 (*C*4a), 134.37 (*C*3'), 133.46 (*C*1), 127.71 (*C*5), 125.07 (*C*3), 124.19 (*C*5a), 123.61 (*C*4'), 123.43 (*C*5'), 121.93 (*C*6'), 121.41 (*C*3a), 120.06 (*C*4), 118.91 (*C*6), 60.67 (*C7a*), 46.77 (*C*9), 36.51 (*C*7), 32.36 (*C*8), 30.26 (*C*7'). MALDI MS (anthracene matrix): calcd *m/z* 525.14 $[\mathbf{M}]^{\bullet+}$, obsd *m/z* 525.14. IR: ν(O-H) 2951 cm^{-1}. Single crystals suitable for X-ray crystallographic analysis were grown by the slow diffusion of hexane into a dichloromethane solution at -30°C under N_2.

[Pt($CH_2CMe_2C_6H_4$)(L2)], 2.

This was prepared similarly from $[Pt_2(CH_2CMe_2C_6H_4)_2(\mu\text{-}SMe_2)_2]$ (0.196 g, 0.252 mmol) and 2-C_5H_4N-CH_2-NH-3-C_6H_4OH, **L2** (0.100 g, 0.504 mmol). Yield: 0.198 g, 0.376 mmol, 75%. NMR in $(CD_3)_2CO$ at 25°C: δ(^{1}H, 600 MHz) 8.81 (d, 1H, *J* = 6 Hz, *H*6a), 8.07 (t, 1H, *J* = 7 Hz, *H*4a), 7.63 (d, 1H, *J* = 7 Hz, *H*3a), 7.45 (dd, 1H, *J* = 6 Hz, 7 Hz, *H*5a), 7.06-7.01 (m, 2H, *H*6, *H*3'), 6.68-6.71 (m, 2H, *H*5, *H*2), 6.64-6.60 (m, 2H, *H*4', H6'), 6.54 (t, 1H, *J* = 7 Hz, *H*4), 6.50 (t, 1H, *J* = 7 Hz, *H*5', 1H), 4.75 (dd, 1H, *J* = 16 Hz, 6 Hz, *H*7a), 4.50 (dd, 1H, *J* = 16 Hz, 5 Hz, *H*7a'), 2.42 (d, 1H, *J* = 9 Hz, $^2J_{PtH}$ = 104 Hz, *H*8), 2.19 (d, 1H, *J* = 9 Hz, $^2J_{PtH}$ = 100 Hz *H*8'), 1.21 (s, 3H, *H*7), 1.20 (s, 3H, *H*7'). δ(^{13}C, 151 MHz) 167.89 (*C*2'), 162.58 (*C*6a), 157.63 (*C*3), 150.31 (*C*4a), 148.15 (*C*2a), 143.44 (*C*1'), 136.84 (*C*2a), 135.13 (*C*6), 129.56 (*C*3'), 124.19 (*C*5a), 122.41 (*C*5' *or C*1), 121.41 (*C*6'), 120.94 (*C*4'), 112.72 (*C*5 *or C*2), 112.04 (*C*4), 109.04

(*C*5 *or C*2), 59.56 (*C*7a), 46.74 (*C*9), 33.87 (*C*7), 32.78 (*C*7'), 27.37 (*C*8). MALDI MS (anthracene matrix): calcd *m/z* 525.14 $[\mathbf{M}]^{\bullet+}$, obsd *m/z* 525.14. IR: ν(O-H) 2920 cm^{-1}.

[Pt($CH_2CMe_2C_6H_4$)(L3)], 3.

This was prepared similarly from $[Pt_2(CH_2CMe_2C_6H_4)_2(\mu\text{-}SMe_2)_2]$ (0.196 g, 0.252 mmol) and 2-C_5H_4N-CH_2-NH-4-C_6H_4OH, **L3** (0.100 g, 0.504 mmol). Yield: 0.187 g, 0.356 mmol, 71%. NMR in $(CD_3)_2CO$ at 25°C: δ(^{1}H, 600 MHz) 9.03 (d, 1H, *J* = 6 Hz, *H*6a), 8.14 (t, 1H, *J* = 7 Hz, *H*4a), 7.68 (d, 1H, *J* = 7 Hz, *H*3a), 7.53 (dd, 1H, *J* = 6 Hz, 7 Hz, *H*5a), 7.17(d, 1H, *J* = 7 Hz, H6'), 7.13 (t, 1H, *H4'*), 7.12 (d, 2H, *J* = 7 Hz, *H*2, *H*6), 6.93 (t, *J* = 6 Hz, NH), 6.73 (d, 2H, *J* = 7 Hz, *H*3, *H*5), 6.71 (t, 1H, *J* = 7 Hz, *H*5'), 6.70 (d, 1H, *J* = 7 Hz, *H*3'), 4.68 (dd, 1H, *J* = 16 Hz, 6 Hz, *H*7a), 4.48 (dd, 1H, *J* = 16 Hz, 6 Hz, *H*7a'), 1.93 (d, 1H, *J* = 9 Hz, *H*8), 1.69 (d, 1H, *J* = 9 Hz, *H*8'), 1.15 (s, 3H, *H*7), 1.05 (s, 3H, *H*7'). δ(^{13}C, 151 MHz) 161.19 (*C*6a), 154.62 (*C*2a), 148.94, 140.25, 136.62, 133.23, 124.35, 122.70 (*C*3, *C*5), 121.49 (*C*5a), 121.12 (*C*3a), 115.12 (*C*2, *C*6), 61.28 (*C*7a), 54.05 (*C*9), 33.65 (*C*7), 32.88 (*C*7'), 26.71 (*C*8). MALDI MS (anthracene matrix): calcd *m/z* 525.14 $[\mathbf{M}]^{\bullet+}$, obsd *m/z* 525.13. IR: ν(O-H) 2920 cm^{-1}.

[Pt($CH_2CMe_2C_6H_4$)(L4)], 4.

To a stirred solution of $[Pt_2(CH_2CMe_2C_6H_4)_2(\mu\text{-}SMe_2)_2]$, (0.196 g, 0.252 mmol) in ether (50 mL) was added a solution of 2-C_5H_4NCH=N-2-C_6H_4OH, **L4** (0.100 g, 0.504 mmol) in ether (20 mL). An immediate color change from yellow to red was observed, and a red precipitate of **4** was formed. After 3h., the product was separated by filtration, washed with hexane (30 mL) and cold acetone (10 mL), and dried under vacuum. Yield: 0.220 g, 0.418 mmol, 83%. NMR in CD_2Cl_2 at -20°C: δ(^{1}H) 9.38 (s, 1H, $^3J_{PtH}$ = 27 Hz, *H*7a), 9.19 (d, 1H, *J* = 6 Hz, *H*6a), 8.15 (t, 1H, *J* = 7 Hz, *H*4a), 7.94 (d, 1H, *J* = 7 Hz, *H*3a), 7.69 (dd, 1H, *J* = 6 Hz, 7 Hz, *H*5a), 7.35 (t, 1H, *J* = 8 Hz, *H*5), 7.28 (d, 1H, *J* = 8 Hz, *H*3), 7.12 (t, 1H, *J* = 8 Hz, *H*4), 6.92 (d, 1H, *J* = 8 Hz, *H*6), 6.83 (m, 2H, *H*3', *H*6'), 6.48 (m, 2H, *H*5', *H*4'), 3.38 (d, 1H, *J* = 12 Hz, $^2J_{PtH}$ = 100 Hz, *H*8), 2.48 (d, 1H, *J* = 12 Hz, $^2J_{PtH}$ = 94 Hz, *H*8'), 1.35 (s, 3H, *H*7), 1.34 (s, 3H, *H*7'). $^{13}C\{^1H\}$ NMR (CD_2Cl_2, 151 MHz, -20°C) δ: 168.55 (*C*2'), 165.46 (*C*7a), 155.60 (*C*2a), 151.62 (*C*2), 149.65 (*C*6a), 141.36 (*C*1'), 138.07 (*C*4a), 137.45 (*C*1), 134.18 (*C*4' *or C*5'), 129.89 (*C*5), 128.51 (*C*5a), 127.96 (*C*3a), 123.75 (*C*3' *or C*6'), 123.39 (*C*4' *or C*5'), 121.51 (*C*3' *or C*6'), 121.06 (*C*3), 120.83 (*C*4), 117.84 (*C*6), 70.82 (*C*8), 47.38 (*C*9), 34.51 (*C*7,*C*7'). At room temperature, the ^{1}H spectrum was similar except that no resonances were observed for the CH_2 protons (*H*8, *H*8') and a single

resonance was observed for the CMe_2 protons of the cycloneophyl group [δ 1.35 (s, 6H, *H*7, *H*7')]. MALDI MS (anthracene matrix): Calc. *m/z* 525.14 $[\mathbf{M}]^{\bullet+}$, obsd *m/z* 525.14. IR: ν(O-H) 2950 cm^{-1}. Single crystals of **4** suitable for X-ray crystallographic analysis were grown by the slow diffusion of hexane into a dichloromethane solution at room temperature.

$[PtCl_2(L4)]$, 5.

To a solution of $[PtCl_2(SMe_2)_2]$ (0.121 g, 0.310 mmol) in CH_2Cl_2 (5 mL) was added ligand **L4** (0.0.061 g, 0.310 mmol). The product **5** formed as an insoluble yellow solid, which was separated, washed with CH_2Cl_2 (2 × 10 mL) and pentane (2 × 10 mL) and dried under vacuum. Yield: 0.105 g, 0.226 mmol, 77%. NMR in $(CD_3)_2SO$: δ(^{1}H, 600 MHz) 10.09 (s, 1H, *H*7a), 9.49 (d, 1H, *J* = 5 Hz, *H*6a), 8.44 (t, 1H, *J* = 7 Hz, *H*4a), 8.23 (d, 1H, *J* = 7 Hz, *H*3a), 8.00 (dd, 1H, *J* = 6 Hz, 7 Hz, *H*5), 7.20-7.24 (m, 2H, *H*4, *H*5), 6.98 (d, 1H, *J* = 7 Hz, *H*6), 6.88 (d, 1H, *J* = 6 Hz, *H*3). δ(^{13}C) 168.23 (*C*2a), 162.29 (*C*7a), 153.05 (*C*2), 151.96 (*C*6a), 149.04 (*C*5a), 140.40 (*C*1), 137.75 (*C*3a), 130.24 (*C*4a), 129.91 (*C*5), 128.90 (*C*4), 126.91 (*C*3), 128.90 (*C*6). Single crystals suitable for X-ray crystallographic analysis were grown by the slow evaporation of a solution in dichloromethane.

$[PtHCl(CH_2CMe_2C_6H_4)(L4)]$, 6.

To a solution of complex **4** (0.040 g, 0.076 mmol) in CD_2Cl_2 (1 mL), in an NMR tube at -60°C, was added HCl generated by reaction of Me_3SiCl (12.5 μL, 0.099 mmol) with H_2O (2 μL, 0.038 mmol) in CD_2Cl_2 (0.5 mL). ^{1}H NMR spectra were recorded at -60, -30, -20, 0 and 25°C. At -60°C, a major hydride resonance was observed at δ −19.62, $^1J_{PtH}$ = 1466 Hz (isomer **6a**) and a less intense resonance at δ −19.51, $^1J_{PtH}$ = 1400 Hz (isomer **6b**). At 0°C, a third hydride resonance was observed at δ −19.17, $^1J_{PtH}$ = 1380 Hz (isomer **6c**), while resonances for isomers **6a** and **6b** decayed. All three isomers were still present at 25°C, and decomposition occurred over a period of several days to give complex **5**.

In a similar reaction, HCl was added to complex **4** in CD_2Cl_2 at room temperature in the presence of 1,3,5-trimethoxybenzene as internal standard. Spectra were recorded immediately (t = 0) and after 15 h. Yields by integration: t = 0, total hydride yield 100%, **6a** 2%, **6b** 80%, **6c** 18%; t = 15 h., total hydride yield 72%, **6a** 2%, **6b** 20%, **6c** 50%. NMR data for **6b** in CD_2Cl_2: δ(^{1}H) 9.67 (d, 1H, *J* = 6 Hz, *H*6a), 9.33 (s, 1H, $^3J_{PtH}$ = 21 Hz, *H*7a), 8.11 (t, 1H, *J* = 7 Hz, *H*4a), 7.98

(dd, 1H, *J* = 6 Hz, 7 Hz, *H*5a), 7.90 (d, 1H, *J* = 7 Hz, *H*3a), 7.40 (d, 1H, *J* = 8 Hz, *H*3), 7.29 (t, 1H, *J* = 8 Hz, *H*4), 7.08 (t, 1H, *J* = 8 Hz, *H*5), 7.00 (d, 1H, *J* = 8 Hz, *H*6), 6.52-6.54 (m, 4H, *H*3'-*H*6'), 3.20 (d, 1H, *J* = 15 Hz, $^2J_{PtH}$ = 72 Hz, *H*8), 2.70 (d, 1H, *J* = 15 Hz, $^2J_{PtH}$ = 70 Hz, *H*8'), 1.53 (s, 3H, *H*7), 1.32 (s, 3H, *H*7'), -19.51 (s, 1H, $^1J_{PtH}$ = 1400 Hz, PtH). IR: ν(PtH) 2290 cm^{-1}. MALDI MS (anthracene matrix): Calcd *m/z* 560.10 $[\mathbf{M\text{-}H}]^+$, Obsd *m/z* 560.11; Calcd *m/z* 525.14 $[\mathbf{M\text{-}HCl}]^+$, Obsd *m/z* 525.14.

[PtHBr($CH_2CMe_2C_6H_4$)(L4)], 7.

This was prepared similarly by reaction of HBr, generated by reaction of Me_3SiBr (13 μL, 0.099 mmol) with H_2O (2 μL, 0.038 mmol), and complex **4** (0.040 g, 0.076 mmol) in CD_2Cl_2 (1.5 mL) at -60°C. The formation of complex **7** was monitored by ^1H NMR as the solution was warmed to room temperature. PtH resonances: **7a** [δ −19.66, $^1J_{PtH}$ = 1453 Hz], **7b** [δ −19.56, $^1J_{PtH}$ = 1395 Hz], **7c** [δ −19.16, $^1J_{PtH}$ = 1356 Hz], with minor isomer **7d** [δ −20.06, $^1J_{PtH}$ = 1444 Hz].

[PtHCl($CH_2CMe_2C_6H_5$)(L1)H], 8.

This was prepared similarly by reaction of HCl, generated by reaction of Me_3SiCl (12.5 μL, 0.099 mmol) with H_2O (2 μL, 0.038 mmol), with complex **1** (0.040 g, 0.076 mmol) in CD_2Cl_2 (1.5 mL) at -60°C. NMR in CD_2Cl_2 at 25°C: δ(PtH) −19.63, $^1J_{PtH}$ = 1340 Hz; -19.90; -20.37, $^1J_{PtH}$ = 1687 Hz; -20.91; -21.13. IR: ν(OH) 3045 cm^{-1} ν(PtH) 2290 cm^{-1}.

Acknowledgments

We thank the NSERC (Canada) for financial support.

References

[1] a) L. Brammer, *Dalton Trans.* **2003**, 3145-3157. b) D. Braga, F. Grepioni, E. Tedesco, K. Biradha, G. R. Desiraju, *Organometallics* **1997**, *16*, 1846-1856. c) E. R. T. Tiekink, *Coord. Chem. Rev.* **2017**, *345*, 209-228. d) A. Martin, *J. Chem. Educ.* **1999**, *76*, 578-583. e) L. R. Falvello, *Angew. Chem. Int. Ed.* **2010**, *49*, 10045-10047.

[2] a) R. J. Puddephatt, *Coord. Chem. Rev.* **2001**, *219-221*, 157-185. b) G. Mazzone, N. Russo, E. Sicilia, *Inorg. Chem.* **2011**, *50*, 10091-10101. c) R. Romeo, G. D'Amico, *Organometallics* **2006**, *25*, 3435-3446. d) G. S. Hill, L. M. Rendina, R. J. Puddephatt,

Organometallics **1995**, *14*, 4966-4968. e) S. S. Stahl, J. A. Labinger, J. E. Bercaw, *J. Am. Chem. Soc.* **1995**, *117*, 9371-9372.

[3] a) M. Lersch, M. Tilset, *Chem. Rev.* **2005**, *105*, 2471-2526. b) J. A. Labinger, J. E. Bercaw, *J. Organomet. Chem.* **2015**, *793*, 47-53. c) E. M. Prokopchuk, H. A. Jenkins, R. J. Puddephatt, *Organometallics* **1999**, *18*, 2861-2866.

[4] a) R. Sanchez-de-Armas, M. S. G. Ahlquist, *Phys. Chem. Chem. Phys.* **2015**, *17*, 812-816. b) O. Kroutil, M. Predota, Z. Chval, *Inorg. Chem.* **2016**, *55*, 3252-3264.

[5] a) M. Baya, U. Belio, A. Martin, *Inorg. Chem.* **2013**, *53*, 189-200. b) J. M. Casas, L. R. Falvello, J. Fornies, A. Martin, A. J. Welch, *Inorg. Chem.* **1996**, *35*, 6009-6014.

[6] A. N. Vedernikov, K. G. Caulton, *Chem. Commun.* **2003**, 358-359.

[7] a) Y.-L. Wong, J.-F. Ma, F. Xue, T. C. W. Mak, D. K. P. Ng, *Organometallics* **1999**, *18*, 5075−5079. b) Y.-L. Wong, D. K. P. Ng, H. K. Lee, *Inorg. Chem.* **2002**, *41*, 5276−5285. c) S. Biswas, K. Mitra, B. Adhikary, C. R. Lucas, *Transition Met. Chem.* **2005**, *30*, 586−592. d) K. Kanamori, K. Kusajima, H. Yachi, H. Suzuki, Y. Miyashita, K.-I. Okamoto, *Bull. Chem. Soc. Jpn.* **2007**, *80*, 324−328.

[8] a) M. E. Moustafa, P. D. Boyle, R. J. Puddephatt, *Chem. Commun* **2015**, *51*, 10334-10336. b) M. A. Fard, A. Behnia, R. J. Puddephatt, *ACS Omega* **2019**, *4*, 257-268. c) M. A. Fard, A. Behnia, R. J. Puddephatt, *ACS Omega* **2018**, *3*, 10267-10272.

[9] M. A. Fard, A. Behnia, R. J. Puddephatt, *Canad. J. Chem.* **2019**, *97*, 238-243.

[10] a) M. A. Fard, A. Behnia, R. J. Puddephatt, *Organometallics* **2018**, *37*, 3368-3377. b) M. A. Fard, A. Behnia, R. J. Puddephatt, *J. Organomet. Chem.* **2019**, *890*, 32-42. c) R. J. Puddephatt, *Canad. J. Chem.* **2019**, *97*, in press, doi.org/10.1139/cjc-2019-0015.

[11] T. G. Appleton, H. C. Clark, L. E. Manzer, *Coord. Chem. Rev.* **1973**, *10*, 335-442.

[12] a) K. A. Grice, M. L. Scheuermann, K. I. Goldberg, *Topics Organomet. Chem.* **2011**, *35*, 1-27. b) R. J. Puddephatt, *Angew. Chem. Int. Ed.* **2002**, *41*, 261-263. c) G. S. Hill, R. J. Puddephatt, *Organometallics* **1998**, *17*, 1478-1486.

[13] a) H. Eyring, *J. Chem. Phys.* **1935**, *3*, 107-115. b) J. Sandstrom, Dynamic Nuclear Resonance Spectroscopy, Academic Press, 1983.

[14] (a) A. D. Becke, *Phys. Rev. A* **1988**, *38*, 3098-3100. (b) ADF 2017, SCM, Vrije Universiteit, Amsterdam, The Netherlands, http://www.scm.com.

10.1002/ejic.201900480

10.1002/ejic.201900480

Key Topic

Platinum-Hydrogen Bonds

Graphical abstract

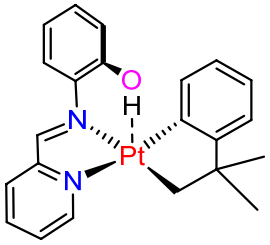

Graphical abstract text

Electron-rich organoplatinum complexes can form intramolecular or intermolecular OH···Pt hydrogen bonds, but formation of hydroplatinum(IV) complexes requires a strong acid such as HCl.

Keywords

Platinum, Hydrogen bond, Hydride ligands, Oxidative addition